one binds via hydrogen bonds (or other weak interactions) near the mouth of the other CD.

It is becoming increasingly evident that cyclodextrin inclusion complexation is not as simple as once believed. It is dangerous to assume a 1:1, 1:2, or 2:1 complex exists without some definitive experimental evidence. For example, this study has shown that two cyclodextrin molecules bind prostaglandin B_1 and B_2 and *p*-nitroaniline while earlier studies assumed 1:1 stoichiometries.[29-31] Obviously, this can significantly alter the interpretation of one's results in studies involving cyclodextrins. For example, rate constants could be significantly altered in going from a 1:1 to a 1:2 complex in catalysis studies involving cyclodextrins. Also the understanding of chiral recognition in cyclodextrin-based systems requires accurate information on both the stoichiometry and conformation of these complexes.

---

(29) Vekama, K.; Hirayama, F.; Ikeda, K.; Inaba, K. *J. Pharm. Sci.* **1977**, *66*, 706.

(30) Vekama, K.; Hirayama, F.; Irie, T. *Chem. Lett.* (*Jpn.*) **1978**, 661.

(31) Kawaguchi, Y.; Tanaka, M.; Nakae, M.; Funazo, K.; Shono, T. *Anal. Chem.* **1983**, *55*, 1852.

Potential Primary Pyrolysis Processes for Disilane

Mark S. Gordon,* Thanh N. Truong, and Elizabeth K. Bonderson

Contribution from the Department of Chemistry, North Dakota State University, Fargo, North Dakota 58105. *Received June 17, 1985*

Abstract: Four competing unimolecular decomposition pathways for disilane are considered with use of MP4 energies obtained with an extended basis set and geometries obtained at the MP2/6-31G** computational level. The 1,1- and 1,2-eliminations of H_2 and the elimination of silylene to form silane all have similar endothermicities, but the very high activation energy for the 1,2-elimination eliminates this process as a significant contributor at low energies. If disilene is formed in the thermal decomposition of disilane, the more likely source is its higher energy isomer silylsilylene via a relatively low energy 1,2-hydrogen shift.

I. Introduction

In the pyrolysis of silane, both trisilane and tetrasilane are detected as final products.[1] An explanation proposed for the appearance of these species is that one of the primary products, silylene (SiH_2), inserts into the parent silane to form disilane. The latter then may itself lose molecular hydrogen to yield silylsilylene (1,1-elimination) or disilene (1,2-elimination). The first of these isomers has been implicated in the subsequent formation of trisilane, while the latter may be the origin of the observed tetrasilane.[1] Alternatively, disilene might be formed via a 1,2-shift from its isomer silylsilylene rather than by direct hydrogen elimination.

It appears to be generally accepted that the primary products in the pyrolysis of disilane result from the molecular elimination of hydrogen or silane.[2] Three such processes, reactions 1-3, are possible:

$$SiH_3{-}SiH_3 \rightarrow SiH_4 + SiH_2 \tag{1}$$

$$SiH_3{-}SiH_3 \rightarrow SiH_3{-}SiH + H_2 \tag{2}$$

$$SiH_3{-}SiH_3 \rightarrow SiH_2{=}SiH_2 + H_2 \tag{3}$$

$$SiH_3{-}SiH_3 \rightarrow SiH_3 + SiH_3 \tag{4}$$

In addition, one can imagine that the Si-Si homolytic cleavage (reaction 4) might be competitive. Of these four reactions, (1) appears to be the dominant primary process,[2] while (4) is less likely due to the 75 kcal/mol required to break the Si-Si single bond.[3] Detection of molecular hydrogen implicates reactions 2 and 3, but it is not clear which of these two reactions is more important. The least motion attack of H_2 on ethylene to form ethane is symmetry forbidden.[4] Because of this, the non-least-motion pathway has a substantial barrier. Even though disilene is nonplanar,[5] one expects a similarly large barrier for reaction 3. In addition to symmetry considerations, the four-center transition state across a rather long Si-Si bond will make delocalized bonding involving all four centers difficult. This should destabilize the transition state relative to the reactants and products. Because of the expected large barrier to the 1,2-elimination, the formation of disilene may well proceed primarily by isomerization from silylsilylene.

This work was initiated primarily to consider the relative thermodynamics and energy barriers for reactions 2 and 3. To place these calculations in the proper perspective, they are compared with reactions 1 and 4. The reverse of reaction 1 has earlier been shown[6] to occur with no barrier, and the same will certainly be true for reaction 4. Improved values for the thermodynamic energy differences for these reactions are presented below. To complete the investigation of the energetically most favorable means for forming disilene, the isomerization process involving the products of reactions 2 and 3 is considered as well.

The molecular and vibrational structure of disilane have been well characterized experimentally,[7] and several theoretical paper concerning this molecule have appeared as well.[8] The first

---

(1) Olbrich, G.; Potzinger, P.; Reimann, B.; Walsh, R. *Organometallics* **1984**, *3*, 1267.

(2) Dzarnoski, J.; Rickborn, S. F.; O'Neal, H. E.; Ring, M. A. *Organometallics* **1982**, *1*, 1217.

(3) Walsh, R. *Acc. Chem. Res.* **1981**, *14*, 246.

(4) Woodward, R. B.; Hoffmann, R. "The Conservation of Orbital Symmetry"; Verlag Chemie: Germany, 1970.

(5) Cowley, A. H. *Polyhedron* **1984**, *3*, 389.

(6) Gordon, M. S.; Gano, D. R. *J. Am. Chem. Soc.* **1984**, *106*, 5421.

(7) Bethke, G. W.; Wilson, E. B., Jr. *J. Chem. Phys.* **1957**, *26*, 1107. Beagley, B.; Conrad, A. R.; Freeman, J. M.; Monaghan, J. J.; Norton, B. G.; Holywell, G. C. *J. Mol. Struct.* **1972**, *11*.

(8) See, for example: Nicolas, G.; Barthelat, J. C.; Durand, P. *J. Am. Chem. Soc.* **1976**, *98*, 1346. Snyder, L. C.; Wasserman, Z. *Chem. Phys. Lett.* **1977**, *51*, 349. Mehandru, S. P.; Ray, N. K. *Indian J. Chem.* **1978**, *16A*, 1. Blustin, P. H.; Dacre, P. D.; Whittaker, C. G. *J. Chem. Soc., Faraday Trans. 2* **1978**, *74*, 982. Moskowitz, J. W.; Topiol, S.; Snyder, L. C.; Ratner, M. A. *Int. J. Quantum Chem.* **1981**, *19*, 131. Xu, J. H.; Mallow, J. V.; Ratner, M. A. *J. Phys. B* **1983**, *16*, 3863. Battistoni, C.; Lapiccirella, A.; Semprini, E.; Stefani, F.; Tomassini, N. *Nuovo Cimento Soc. Ital. Fis.* **1984**, *3D*, 663.

0002-7863/86/1508-1421$01.50/0

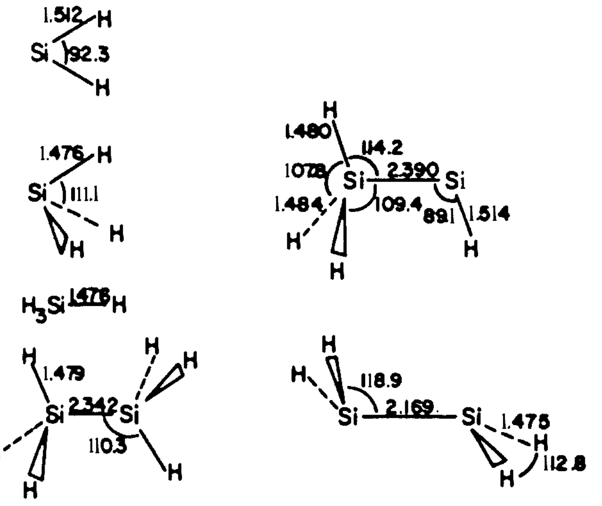

Figure 1. Structures of stable species. Bond lengths in Å, angles in deg.

compounds containing silicon–silicon double bonds were synthesized by the groups of West and Michl,[9] Masamune,[10] and Boudjouk.[11] While the unsubstituted molecule is apparently nonplanar, West[12] has suggested several substituents that may planarize the structure.

The early theoretical papers on disilene and its isomers have recently beeen reviewed by Cowley.[5] Accurate ab initio calculations predict the parent disilene structure to be slightly bent, in agreement with the X-ray structure.[9] Even so, the Si–Si bond length is considerably shorter than that in disilane, suggesting substantial π bonding. Indeed, Potzinger, Walsh, and co-workers[1] have recently calculated the π bond strength in disilene to be 22 kcal/mol, about half that in silaethylene,[13] but still substantial.

The relative energies of disilene and its isomer silylsilylene appears to be rather sensitive to the level of theory used. At the Hartree–Fock level, the silylene is predicted to be lower by 2–9 kcal/mol, depending on the size of the basis set.[14,15] Addition of d functions to the silicon[15] tends to reduce the energy difference. Addition of correlation corrections continues this trend. Poirier and Goddard,[16] using the 3-21G basis set,[17] augmented by singles and doubles configuration interaction (CI), predict disilene to be lower by 8–10 kcal/mol. The more accurate calculation by Krogh-Jespersen,[18] using MP3[19] /6-31G**[20] wave functions at MP2/6-31G* geometries, finds disilene to be more stable by 5 kcal/mol. All recent ab initio calculations agree that the ground states of both isomers are closed-shell singlets.

II. Computational Approach

All molecular structures, including those for transition states, were determined by using the search methods in GAUSSIAN80[21] and GAUSSIAN82,[22] with RHF wave functions except as noted below. Preliminary geometry calculations were performed with the 3-21G,[17] 6-31G*,[20] and 6-31G**[20] basis sets with SCF wave functions. The final structures were all calculated with the latter basis set and with second-order perturbation theory corrections (MP2[19]/6-31G**). At each of the final structures, single-point calculations were carried out with extended basis sets and higher levels of perturbation theory. For hydrogen, the extended basis set was chosen to be -311G**.[23] For silicon, the McLean–Chandler[24] extended basis, augmented by a single set of six d functions (exponent = 0.395),[20] was used.

Single-point calculations for the stable species were performed with use of MP4 (SDTQ)[25] level wave functions. Because the transition state for reaction 2 has no symmetry, a full MP4 calculation at this level would have been prohibitive. For example, for the Si_2H_4 isomerization transition state, the MP4/MC-311G** single-point calculation with and without triples required 1.5 and 5.5 CPU hours on an IBM 3081/D. So, all activation barriers, except that for the isomerization, were calculated at the MP4(SDQ)/MC-311G** level. To investigate the relative importance of a multiconfigurational description of the two Si_2H_4 isomers, single-point MCSCF calculations were performed on these species with use of a modified version of GAMESS.[28] To provide a more direct comparison with experimentally determined energies, zero-point vibrational corrections have been added to the calculated electronic energies by using harmonic frequencies calculated at the optimal geometries, using 6-31G** SCF force fields.

Table I, Predicted Harmonic Frequencies (cm^{-1})

Disilane[a]					
A_{1g}:	2353 (2152):	SiH stretch	A_{1u}:	91:	torsion
	1025 (909):	SiH_3 bend	A_{2u}:	2339 (2154):	Si–H stretch
	472 (434):	Si–Si stretch		940 (843):	SiH_3 bend
E_u:	2349 (2179):	SiH stretch	E_g:	2339 (2155):	Si–H stretch
	1037 (940):	SiH_3 def		1022 (929):	SiH_3 def
	398 (379):	SiH_3 rock		689 (625):	SiH_3 rock
Disilene					
A_g:	2369:	Si–H stretch	B_g:	2375:	Si–H stretch
	1035:	SiH_2 stretch		660:	SiH_2 def
	608:	Si–Si stretch	B_u:	2359:	Si–H stretch
	335:	out-of-plane bend		985:	SiH_2 rock
A_u:	2369:	Si–H stretch		527:	SiH_2 bend
	574:	scissor			
	373:	SiH_2 twist			

[a] Experimental values (Bethke, G. W.; Wilson, E. B. *J. Chem. Phys.* **1951**, *26*, 1107) in parentheses.

Table II. Energetics for Disilane Decomposition[a] (kcal/mol)

	energy differences				
products	MP2	MP3	MP4-(SDQ)	MP4-(SDTQ)	Δ*H*(MP4, SDTQ)
$SiH_4 + SiH_2$	56.3	54.5	52.9	54.0	50.0
$SiH_3Si + H_2$	61.5	60.1	58.9	59.2	53.4
$SiH_2SiH_2 + H_2$	54.1	54.2	53.7	52.2	47.0
$2SiH_3$	73.4	73.9	73.1	74.3	70.0
	barriers				
products	MP2	MP3	MP4-(SDQ)	MP4-(SDTQ)	E_a(MP4, SDQ)
$SiH_3SiH + H_2$	57.3	57.3	57.7		55.5
$SiH_2SiH_2 + H_2$	88.5	88.7	89.0		86.1
$SiH_3SiH \rightarrow SiH_2SiH_2$		11.2	11.9	9.9	9.0

[a] All results obtained with use of the MC-311G** basis set.

---

(9) West, R.; Fink, M. J.; Michl, J. *Science* **1981**, *214*, 1344. Fink, M. J.; Michalczyk, M. J.; Haller, D. J.; West, R.; Michl, J. *J. Chem. Soc., Chem. Commun.* **1983**, 1010.

(10) Masamune, S.; Hanazawa, Y.; Murakami, S.; Bally, T.; Blount, J. F. *J. Am. Chem. Soc.* **1982**, *104*, 1150.

(11) Boudjouk, P.; Han, B.; Anderson, K. R. *J. Am. Chem. Soc.* **1982**, *104*, 4992.

(12) West, R. Seventh International Symposium on Organosilicon Chemistry, Kyoto, Japan, Sept 1984.

(13) Schmidt, M. W.; Gordon, M. S.; Dupuis, M. *J. Am. Chem. Soc.* **1985**, *107*, 2585.

(14) Snyder, L. C.; Wasserman, Z. *J. Am. Chem. Soc.* **1979**, *101*, 5222.

(15) Lischka, H.; Kohler, H.-J. *Chem. Phys. Lett.* **1982**, *85*, 467.

(16) Poirier, R. A.; Goddard, J. D. *Chem. Phys. Lett.* **1981**, *80*, 37.

(17) Binkley, J. S.; Pople, J. A.; Hehre, W. J. *J. Am. Chem. Soc.* **1980**, *102*, 939. Gordon, M. S.; Binkley, J. S.; Pople, J. A.; Pietro, W. J.; Hehre, W. J. *J. Am. Chem. Soc.* **1984**, *106*, 2797.

(18) Krogh-Jespersen, K. *J. Phys. Chem.* **1982**, *86*, 1492.

(19) Binkley, J. S.; Pople, J. A. *Int. J. Quantum Chem.* **1975**, *9*, 229. Pople, J. A.; Binkley, J. S.; Krishnan, R. *Int. J. Quantum Chem. Symp.* **1976**, *10*, 1.

(20) Hariharan, P. C.; Pople, J. A. *Theor. Chim. Acta* **1973**, *28* 213. Gordon, M. S. *Chem. Phys. Lett.* **1980**, *76*, 163.

(21) Binkley, J. S.; Whiteside, R. A.; Seeger, R.; DeFrees, D. J.; Schlegel, H. B.; Topiol, S.; Kahn, L. R.; Pople, J. A. *QCPE* **1981**, *13*, 406.

(22) Binkley, J. S.; Frisch, M. J.; DeFrees, D. J.; Krishnan, R.; Whiteside, R. A.; Schlegel, H. B.; Fluder, E. M.; Pople, J. A. "GAUSSIAN82"; Carnegie-Mellon University: Pittsburgh, PA, 1983.

(23) Krishnan, R.; Binkley, J. S.; Seeger, R.; Pople, J. A. *J. Chem. Phys.* **1980**, *72*, 650.

(24) McLean, A. D.; Chandler, G. S. *J. Chem. Phys.* **1980**, *72*, 5639.

(25) Krishnan, R.; Pople, J. A. *Int. J. Quantum Chem.* **1978**, *14*, 91.

(26) Dupuis, M.; Spangler, D.; Wendoloski, J. J. NRCC Cat. Prog. QGO1, 1980.

(27) The various approaches to the intrinsic reaction coordinate are reviewed in ref 13.

(28) Foster, J. M.; Boys, S. F. *Rev. Mod. Phys.* **1963**, *32*, 300.

Table III. Vibrational Frequencies (cm^{-1})

A. SiH_2 (C_{2v}):	1120 (a_1, bend) 2183 (b_2, antisym str) 2194 (a_1, sym str)
B. SiH_3 (C_{3v}):	857 (a_1, bend) 1010 (e, bend) 2344 (a_1, sym str) 2365 (e, degenerate str)
C. SiH_4 (T_d):	1007 (t_2, bend) 1047 (e, bend) 2367 (t_2, str) 2374 (a_1, str)
D. SiH_3SiH:	134 (a″, internal rot) 419 (a′, Si–Si str, bend) 427 (a″, bend) 473 (a′, Si–Si str, bend) 790 (a′, bend) 971 (a′, bend) 1016 (a′, bend) 1036 (a″, bend) 2175 (a′, SiH str) 2314 (a′, SiH_3 str) 2315 (a″, SiH_3 str) 2337 (a′, SiH_3 str)

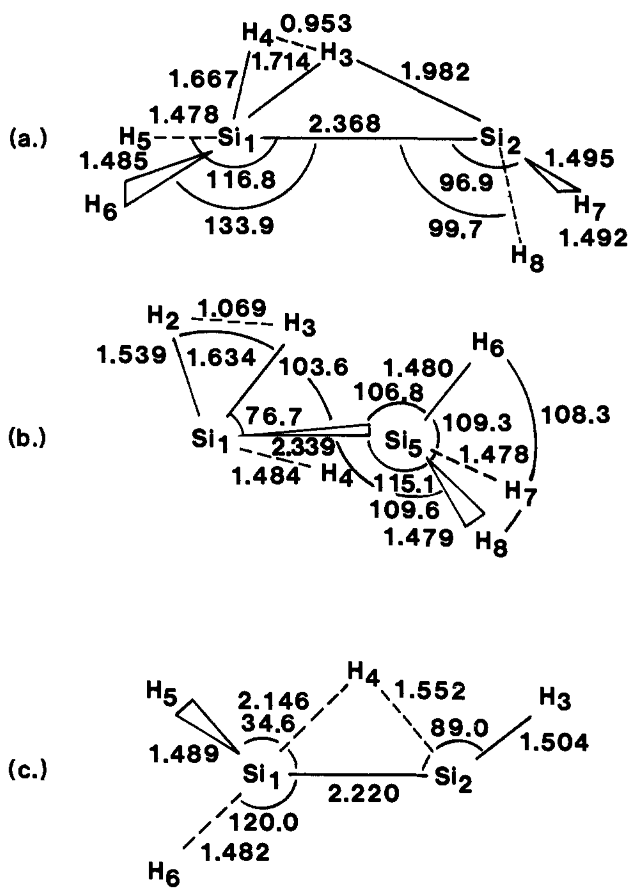

Figure 2. Structures of transition states. Bond lengths in A, angles in deg. (a) Dihedral angles are 4-3-2-1 = 14.8, 5-1-2-3 = 85.7, 6-1-2-3 = −97.4, 7-2-1-3 = 109.7, 8-2-1-3 = −143.9. (b) Angles 4-1-2 and 4-1-3 are 101.7 and 85.3, respectively. Dihedral angle 6-5-1-4 = 139.8. (c) Dihedral angles are 4-1-2-3 = 99.2, 5-1-2-3 = −21.5, 6-1-2-3 = 156.0.

For reaction 3 and the Si_2H_4 isomerization, the intrinsic reaction coordinate (IRC)[13,27] connecting the reactants, transition state, and products was generated and the progress of the reactions monitored by using Boys localized orbitals.[28]

III. Results and Discussion

A. Molecular Structures. The MP2/6-31G** geometries of the stable structures (i.e., those with positive definite force constant matrices) considered in this work are displayed in Figure 1. The structures of the known compounds silane[29] and disilane[7] are in excellent agreement with experiment, with the bond lengths and angles in agreement to within 0.01 Å and 1°, respectively. The Si–Si bond in silylsilylene is somewhat longer than that in disilane, while that in disilene is much shorter. Despite this indication of substantial π bonding, unsubstituted disilene is found to be slightly nonplanar. This is consistent with the X-ray structure[9] and with the results of previous calculations.[14-16]

The vibrational frequencies for disilane and disilene, calculated with 6-31G** SCF wave functions at the MP2 geometries, are listed in Table I, and those for the remaining stable species are given in Table III. As expected for vibrational frequencies calculated at this level, the predicted values for disilane are about 10% higher than the experimental ones. One expects a similar level of agreement for disilene.

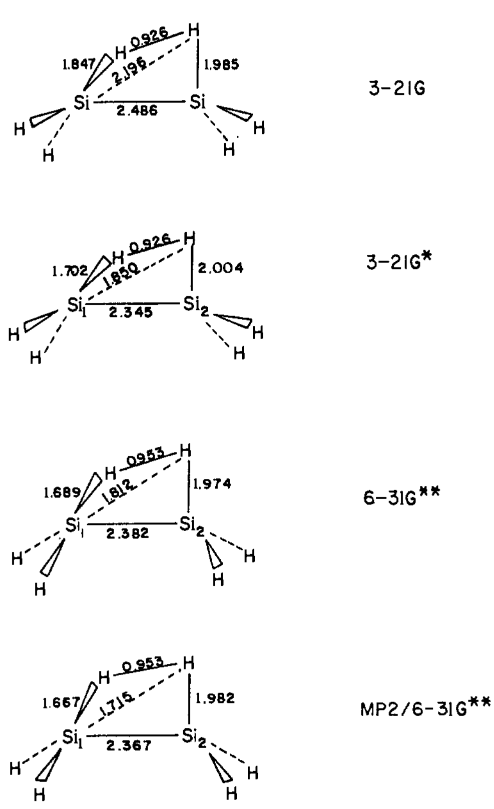

Figure 3. Transition state structure for $H_2 + SiH_2{=}SiH_2$ as a function of computational level. Bond lengths in A, angles in deg.

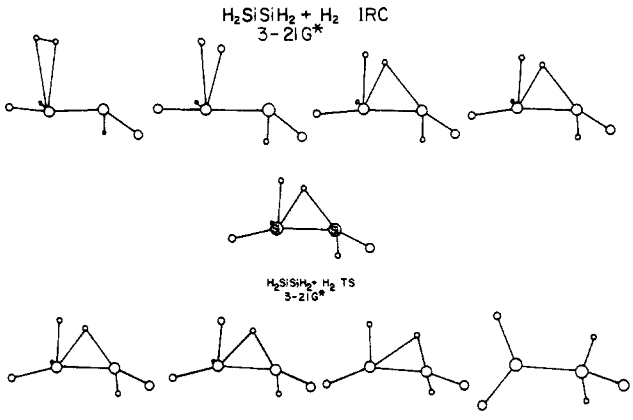

Figure 4. Schematic of structural changes along the $H_2 + SiH_2{=}SiH_2$ intrinsic reaction coordinate.

---

(29) Calloman, J. H.; Hirota, E.; Kuchitsu, K.; Lafferty, W. J.; Maki, A. G.; Pote, C. S. "Structural Data on Free Polyatomic Molecules"; Landolt-Bornstein, New Sciences Group II, Hellwegge, K. H., Hellwegge, A. M., Eds.; Springer-Verlag: Berlin, 1976; Vol. 7.

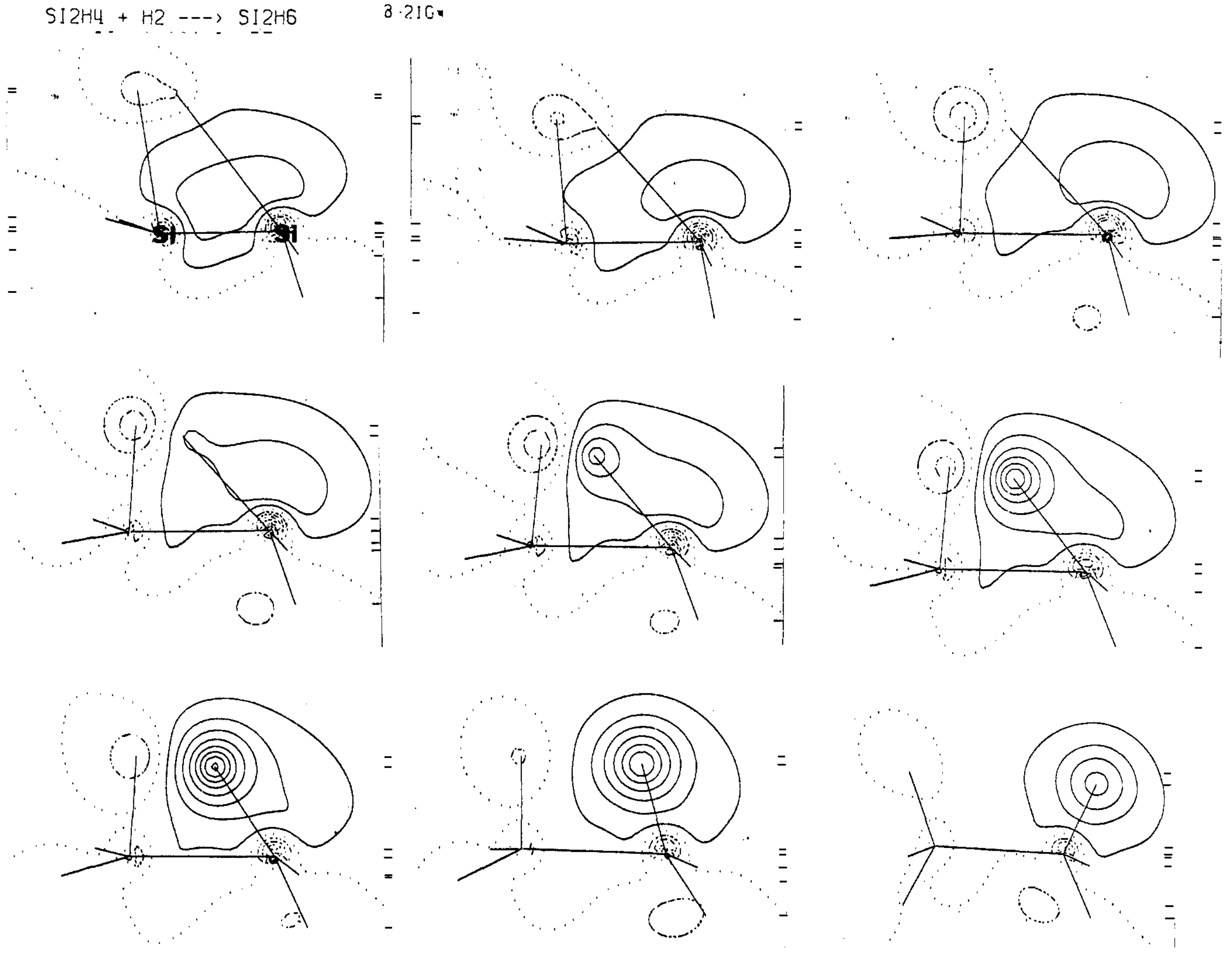

Figure 5. Transformation of Si–Si bond into Si–H bond along the H_2 + $SiH_2{=}SiH_2$ IRC.

The structures for the three transition states which remain at the MP2/6-31G** level are displayed in Figure 2. The structure for the 1,2-hydrogen elimination reaction is the most interesting, since the Si–Si bond is longer than that at both reactant and products, and both reacting hydrogens are closer to one of the silicons. The importance of polarization functions and correlation on the details of this structure is analyzed in Figure 3. The most important of these effects is clearly the addition of d orbitals to silicon, without which the reacting hydrogens are predicted to be between the two silicons. Starting from the 3-21G* transition structure, the intrinsic reaction coordinate for this reaction has been traced to both reactants and products. The resulting structures are displayed schematically in Figure 4. Viewed as an addition reaction, the initial approach of H_2 appears to form a silane–silylene complex. Only after the transition state is passed does one hydrogen move toward the second silicon. This suggests that the π bond (or one of the two Si–Si banana bonds) is first transformed into a lone pair and only later into an Si–H bond.

The foregoing analysis may be verified by considering the Boys localized orbitals along the IRC. These are shown in Figures 5–7. In all three figures, the center frame is the transition state. At large interfragment distances, the orbital in Figure 5 is one of two Si–Si banana bonds. As the hydrogen molecule approaches disilene, this orbital distorts toward the silicon atom on the right, and as suggested above, the structure takes on the appearance of a silane–silylene complex, with the silylene lone pair roughly pointing at the closest hydrogen. As H_2 moves in further, the orbital increasingly takes on the character of the Si–H bond being formed. Figure 6 depicts the other banana bond along the same path. Here, there is simply a small distortion as the orbital becomes the Si–Si σ bond in disilane. Finally, Figure 7 shows the transformation of the H–H bond into the remaining new Si–H bond.

B. Energetics. The energetics for the disilane decomposition reactions are summarized in Table II and Figure 8. All of these calculations have been carried out with the MC-31G** basis set. It is clear from Table II that there is very little variation in either the predicted energy differences or the energy barriers as the level of perturbation theory is increased. The largest effect of triple excitations at the MP4 level is the 2-kcal/mol reduction in the barrier for the 1,2-hydrogen shift from silylsilylene to disilene. A similar reduction is expected for the other barriers, and this is not expected to change the essential features presented here. In order to maintain consistency, the values used in Figure 8 are those obtained from MP4(SDQ), with zero-point corrections included.

Thermodynamically, all three molecular eliminations are found to be competitive, with predicted reaction enthalpies calculated to be within a 6-kcal/mol range. The value obtained for the silylene elimination to form silane (reaction 1) is in good agreement with that estimated by Ring and O'Neal.[2] The products disilene + H_2 (reaction 3) are actually found to be slightly lower in energy, after zero-point corrections, with silylsilylene + H_2 slightly higher. The highest energy process involving Si–Si bond breaking is the homolytic cleavage to form two silyl radicals (reaction 4). The predicted ΔH for this reaction is about 4 kcal/mol below the experimental value.[3] Breaking an Si–H bond is expected to cost about 10 kcal/mol more.

The calculated energy barriers have a dramatic effect on the foregoing results. As expected from the earlier discussion, the 1,2-elimination of H_2 to form disilene requires surmounting a large (86.1 kcal/mol) activation energy. In contrast, the reverse of

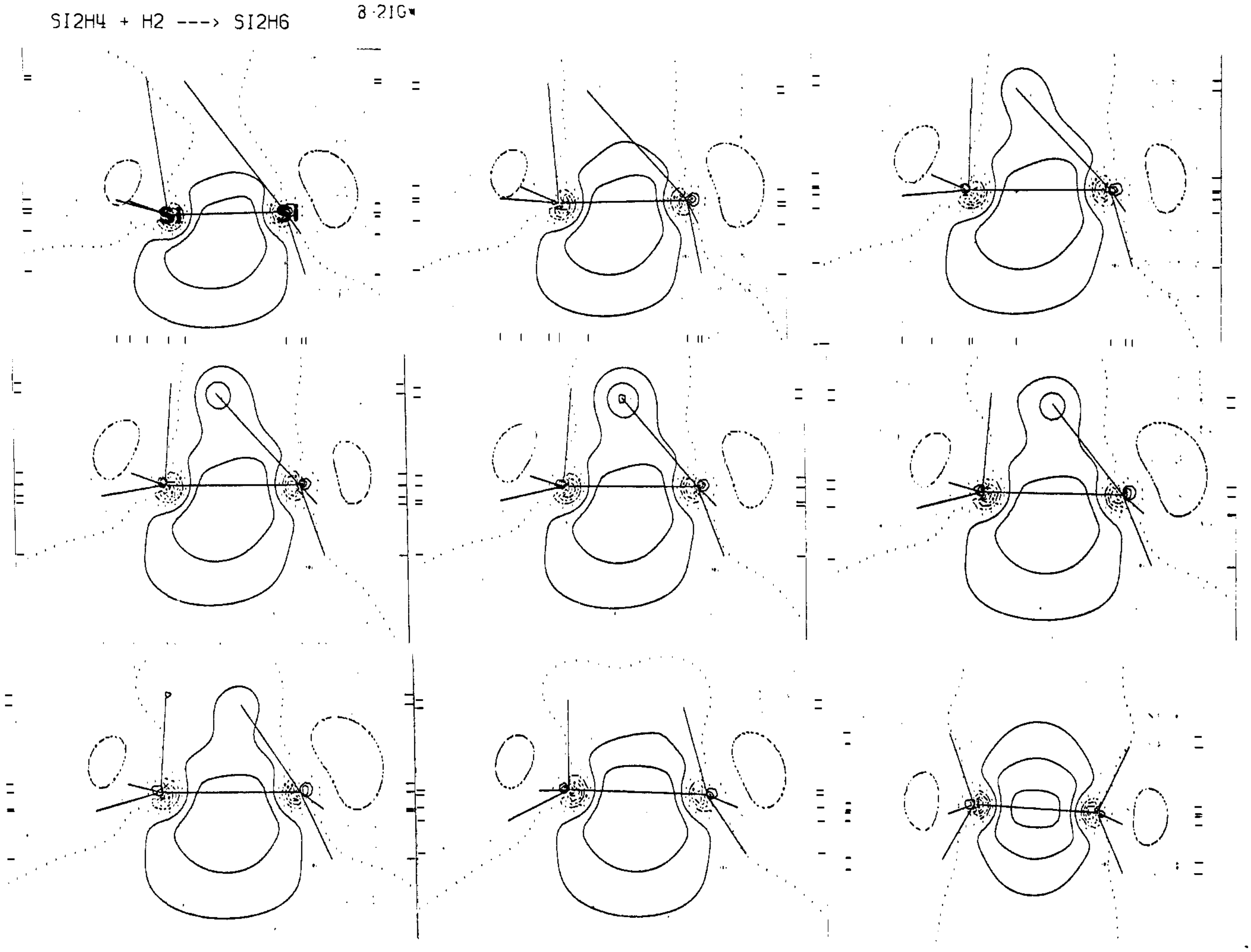

Figure 6. Transformation of Si–Si banana bond in Si–Si σ bond along the H_2 + $SiH_2{=}SiH_2$ IRC.

reaction 1 occurs with no barrier;[6] thus, the observed production of silane is clearly favored kinetically. Indeed, it is clear from Figure 8 that if disilene is produced in silane or disilane pyrolysis, the most likely route is via isomerization from silylsilylene. The latter reaction is predicted to have an activation energy of only 9 kcal/mol. Combined with the 55.5 kcal/mol activation energy for the production of H_3SiSiH (in good agreement with the experimental value of 56.5 kcal/mol[2]), the overall energy requirement for this route to disilene is 21.6 kcal/mol less than that for the direct 1,2-elimination.

Note that, before the addition of zero-point corrections, the barrier for the 1,1-H_2 elimination is actually slightly below the separated products. Since the force constant matrix at the transition state for this reaction has just one negative eigenvalue and the normal mode corresponding to the imaginary frequency clearly corresponds to the 1,1-elimination, this suggests that this reaction has a long-range minimum corresponding to a loosely bound complex between silylsilylene and H_2. A similar complex has been found for the silane decomposition.[30]

Disilene is predicted to be 6.4 kcal/mol lower in energy than its silylene isomer. Because the lowest lying unoccupied orbitals of silylenes are often rather low in energy, it is important to investigate whether a single configuration-based calculation on these two isomers is biased in favor of the disilene isomer. Consequently, a four-electron, four-orbital FORS-MCSCF[31] / 6-31G* calculation was performed on each isomer, such that all orbitals involved in Si–Si bonding have been correlated. While the silylene is lower in energy at the SCF level, incorporation of correlation reverses the order, just as it does using the perturbation theory corrections. The calculated energy difference at the MCSCF level is 3.9 kcal/mol. For both isomers, the natural orbital occupation numbers n_i for σ and σ^* orbitals are 1.98 and 0.02, respectively. For disilene, n_i for π and π^* are 1.86 and 0.14, respectively, while the corresponding values for the lone pair and "empty" p orbitals of the silylene are 1.92 and 0.08. Thus, correlation of the double bond in disilene is more important than HOMO–LUMO correlation in the silylene.

Finally, we find, at the MP4(SDTQ)/MC-311G** level of accuracy, that the energy required to dissociate disilene into two silylenes is predicted to be 56.7 kcal/mol, more than 13 kcal/mol *less* than that for dissociation of disilane into two silyl radicals. This is the reverse of that found for ethylene vs. ethane[32] and reflects both the reduced strength of the Si=Si double bond and the unusual stability of silylene.

IV. Conclusions

The major conclusion to be drawn from this work is that while the three competing molecular eliminations from disilane have similar thermodynamic energetics, the 1,2-elimination of H_2 requires a very large barrier. As a result, the most likely products are silylene and silane (in agreement with experiment). The most likely route to disilene is production of its less stable isomer silylsilylene, followed by a 1,2-hydrogen shift.

Finally, it is worthwhile to speculate on the effects that further improvements in the computational level are likely to have on the calculated results. Recent calculations on the insertion of silylene

---

(30) Gordon, M. S.; Binkley, J. S.; Frisch, M. J.; Gano, D. R. *J. Am. Chem. Soc.*, in press.

(31) Ruedenberg, K.; Schmidt, M. W.; Gilbert, M. M.; Elbert, S. T. *Chem. Phys.* **1982**, *71*, 41. Ruedenberg, K.; Schmidt, M. W.; Gilbert, M. M. *Chem. Phys.* **1982**, *71*, 51. Ruedenberg, K.; Schmidt, M. W.; Gilbert, M. M.; Elbert, S. T. *Chem. Phys.* **1982**, *71*, 65.

(32) Gordon, M. S., unpublished results.

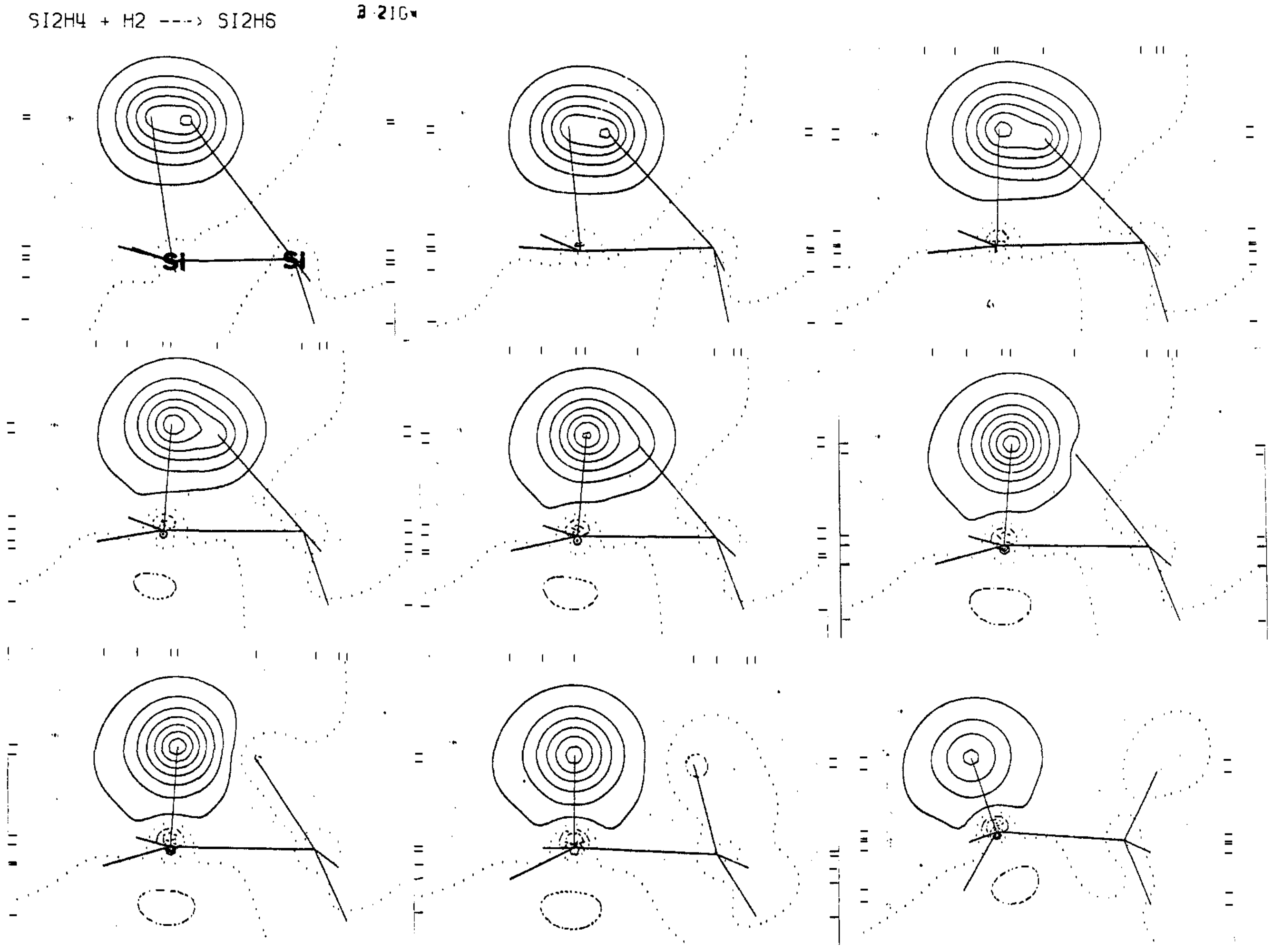

Figure 7. Transformation of H-H bond into Si-H bond along the H_2 + $SiH_2{=}SiH_2$ IRC.

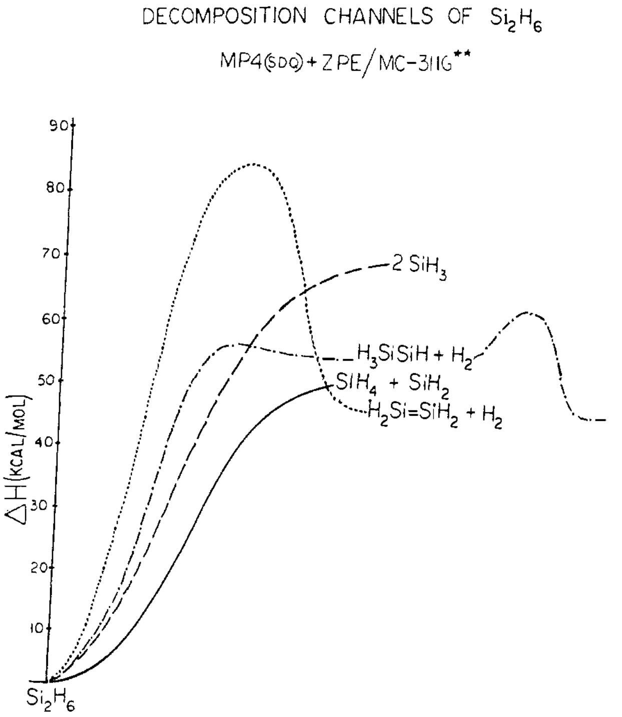

Figure 8. Schematic of disilane potential energy surface, from MP4(SDQ)/MC-31G** with zero-point corrections.

into H_2[30] will aid in this analysis. FORS/MCSCF calculations at several points along that surface verified that the insertion process is well represented with a single configuration based wave function, since very little mixing was observed. It is expected that the analogous insertion of silylsilylene will behave similarly. For the 1,2-addition, the two adding hydrogens are in fact closer to each other than in the 1,1-insertion. Thus, one would expect this structure to be well behaved also. Two additional indications of this are the very small renormalization constant required for the first-order wave function and the fact that the RHF solution is stable at the 1,2-transition state. It is possible that the latter will not be true for all points along the IRC; however, it is unlikely that the qualitative illustrations in Figures 4–7 will change significantly.

For the silane surface[30] further improvement of the basis set beyond MC-311G**, by adding an second set of polarization functions as well as f and d functions to heavy and hydrogen atoms, respectively, and diffuse functions to all atoms reduced the insertion barrier by 4 kcal/mol and increased the exothermicity by 1 kcal/mol. Similar effects are expected for the silylsilylene insertion discussed here. The addition of triple excitations to the fourth-order perturbation corrections is expected to lower the barrier by an additional 1–2 kcal/mol. Because improvements in the wave function consistently lower the energy of disilene relative to silylsilylene, further improvements in the basis set are likely to increase the predicted energy difference between these isomers by more than just 1 kcal/mol—possibly by as much as 5 kcal/mol. This, in turn, will further reduce the barrier for the isomerization and will probably cause comensurate changes in the energetics for the 1,2-elimination. Because the barrier for the latter is so large, it is unlikely that the major conclusions drawn here will be affected.

Acknowledgment. This work was supported by the donors of the Petroleum Research Fund, administered by the American

Chemical Society, and by the National Science Foundation (CHE8309948). The computer time used in this work was provided by the North Dakota State University Computer Center and by the IBM Research Center at Yorktown Heights. The author also benefitted from discussions with Professor S. Nagase of Yokohama National University, Dr. Michael W. Schmidt of North Dakota State University, and Dr. J. S. Binkley at Sandia National Laboratory.

Registry No. SiH_3-SiH_3, 1590-87-0.

Trinuclear Zr_2,Al μ-Ketene Complexes Containing Bridging Ligands. Implications for Transmetallation Reactions and CO Reduction Chemistry[†]

Robert M. Waymouth, Bernard D. Santarsiero, Robert J. Coots, Michael J. Bronikowski, and Robert H. Grubbs*

Contribution No. 7192 from the Laboratories of Chemistry, California Institute of Technology, Pasadena, California 91125. *Received June 18, 1985*

Abstract: A family of ketene–alkylaluminum complexes of formula $[(\eta^5\text{-}C_5H_5)_2Zr(C,O\text{-}\eta^2\text{-}OCCHR)]_2(\mu\text{-}AlR'_2)(\mu\text{-}X)$ has been prepared by treating the zirconocene ketene complexes $[(\eta^5\text{-}C_5H_5)_2Zr(C,O\text{-}\eta^2\text{-}OCCHR)]_2$ with alkylaluminum reagents R'_2AlX (II, III, R = CH_2CMe_3, R′ = Me, X = Me; VIa, VIIa, R = CH_2CMe_3, R′ = CH_3, X = Cl; VIIb, R = H, R′ = CH_3, X = Cl; IX, X, R = CH_2CMe_3, R′ = Et, X = H). The crystal and molecular structure of four compounds of this series (III, VIIa, IX, and X) have been determined. Complex VIIa crystallizes in space group $P2_1/c$ ($Z = 4$) with cell constants a = 10.2193 (14) Å, b = 20.237 (3) Å, c = 18.458 (3) Å, β = 94.303 (14)°, and V = 3802.8 (10) Å^3 (3567 reflections, R = 0.053). Complex IX crystallizes in space group $C2/c$ ($Z = 8$) with cell constants a = 11.777 (5) Å, b = 19.998 (4) Å, c = 32.636 (11) Å, β = 96.83 (5)°, V = 7631.8 (2) Å^3 (4989 reflections, R = 0.067). Complex X crystallizes in space group $C2/c$ (Z = 4) with cell constants a = 18.219 (2) Å, b = 10.364 (1) Å, c = 20.273 (2) Å, β = 94.565 (8)°, and V = 3816 (1) Å^3 (2845 reflections, R = 0.049). Structural comparisons of these molecules reveal several common features. Two zirconocene ketene monomers are spanned by symmetric dialkylaluminum and hydride, chloride, or methyl bridges to form slightly puckered six-membered rings. A notable feature of these structures is the coordination of the bridging ligand X (H, Cl, or Me), which is characterized by a large M–X–M angle and an unusual hybridization for the bridging methyl ligand. The coordination of the bridging methyl group in III represents a new bonding geometry for carbon. This geometry models the structure of intermediates in alkyl transmetallations that proceed with inversion. The reaction of III with acetylene produces a zirconocene cyclic enolate IV. Complex III also reacts with carbon monoxide to produce a zirconocene acyl–enol complex V—an unprecedented reaction for Group 4 ketene complexes that is relevant to the behavior of such species over early transition-metal Fischer–Tropsch catalysts. The greater reactivity of III is discussed in terms of the greater lability of the methyl bridge compared to the chloride or hydride bridge.

Transition-metal ketene complexes have been implicated as intermediates in heterogeneous CO reduction[1] and have been demonstrated to be involved in stoichiometric CO reduction processes.[2,4d] Ketene complexes also show considerable promise as intermediates in organic synthesis.[3] We have recently developed an efficient and general route to early transition-metal ketene complexes.[4] Deprotonation of Group 4 acyl halide metallocenes[5] cleanly affords ketene complexes in high yield (eq 1).[6]

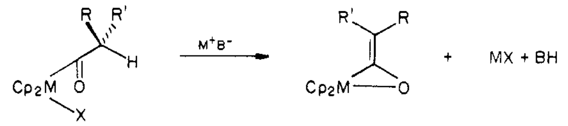

(1)

The monomeric bis(η^5-pentamethylcyclopentadienyl)zirconocene ketene complexes and oligomeric bis(η^5-cyclopentadienyl)titanocene ketene complexes prepared by this route are reactive toward olefins and other substrates under mild conditions.[4a,d] We envisioned that an olefin or acetylene insertion reaction might be synthetically useful if applied to the readily prepared bis(η^5-cyclopentadienyl)zirconocene ketene complexes (eq 2).[7] However,

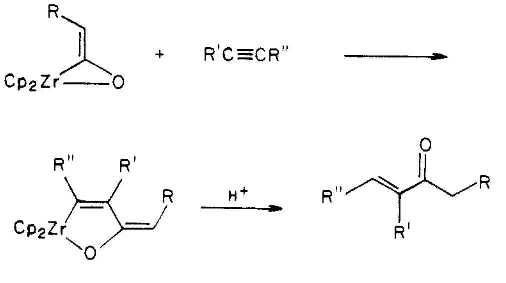

(2)

[†] In this paper, the periodic group notation is in accord with recent actions by IUPAC and ACS nomenclature committees. A and B notation is eliminated because of wide confusion. Groups IA and IIA become groups 1 and 2. The d transition elements comprise groups 3 through 12, and the p block elements comprise groups 13 through 18. (Note that the former Roman numeral designation is preserved in the last digit of the new numbering, e.g., III → 3 and 13.)

(1) (a) Blyholder, G.; Emmet, P. H. *J. Phys. Chem.* **1960**, *64*, 470. (b) Ichikawa, M. B.; Sekizawa, K.; Shikakura, K.; Kawai, M. *J. Mol. Catal.* **1981**, *11*, 167. (c) Takeuchi, A.; Katzer, J. R. *J. Phys. Chem.* **1982**, *86*, 2438.

(2) (a) Barger, P. T.; Santarsiero, B. D.; Armantrout, J.; Bercaw, J. E. *J. Am. Chem. Soc.* **1984**, *106*, 5178 and references therein. See also: (b) Wolczanski, P. T.; Bercaw, J. E. *Acc. Chem. Res.* **1980**, *13*, 121. (c) Morrison, E. D.; Steinmetz, G. R.; Geoffroy, G. L.; Fultz, W. C.; Rheingold, A. L. *J. Am. Chem. Soc.* **1984**, *106*, 4783 and references therein. (d) Miyashita, A.; Grubbs, R. H. *Tetrahedron Lett.* **1981**, 1255. Miyashita, A. Abstracts of papers submitted to 3rd China-Japan-US Symposium on Organometallic Chemistry and Catalysis, Santa Cruz, CA, August 5, 1984.

(3) (a) Dotz, K. H. *Pure Appl. Chem.* **1983**, *55*, 1689. (b) Semmelhack, M. F.; Tamura, R.; Schnatter, W.; Springer, J. *J. Am. Chem. Soc.* **1984**, *106*, 5363.

0002-7863/86/1508-1427$01.50/0